Supplementary Figures

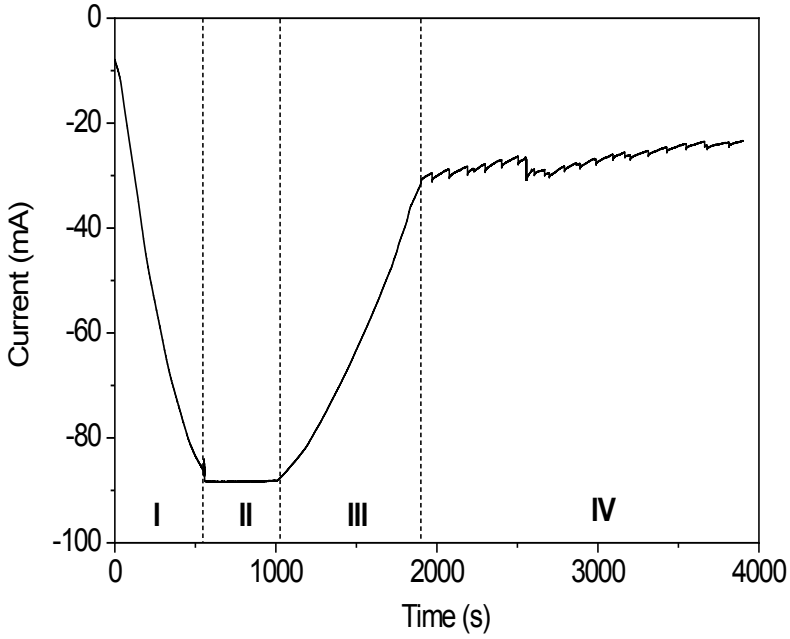

Figure S1. I-t curve for reduction of r-Cu_{ox}(350) at −0.70 V *vs*. RHE in 0.1 M $KHCO_3$. Phase I indicates that reduction begins at the Cu_{ox}(350) surface to the bulk; Phase II indicates the achievement of the maximum reductive current; Phase III indicates the end of reduction ; Phase IV indicates the beginning of HER.

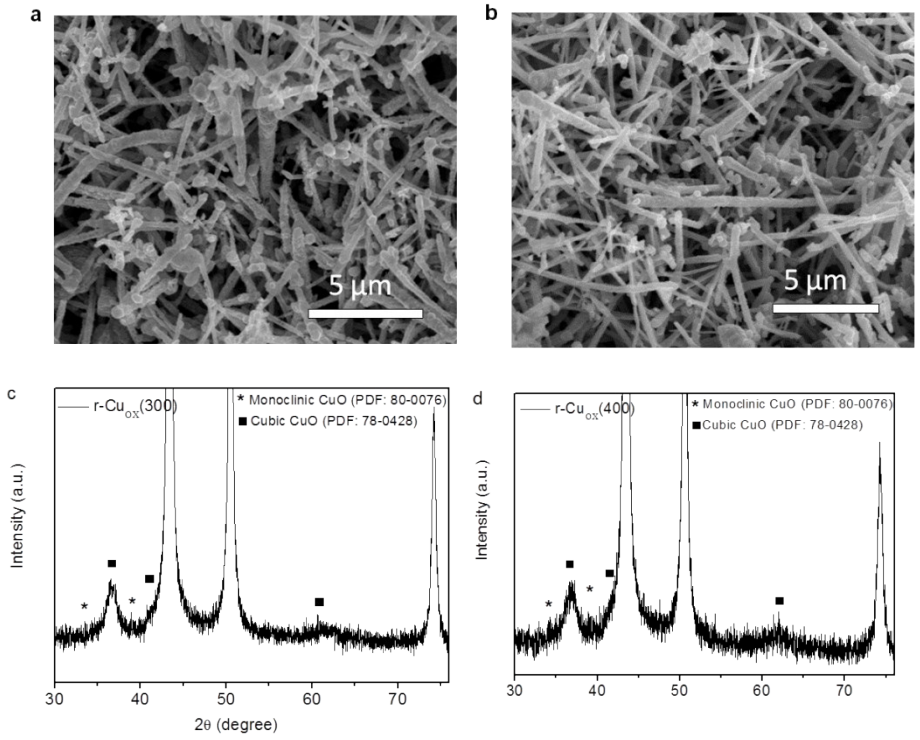

Figure S2. (a,b) SEM images and (c,d) XRD patterns of the r-Cuox(300) and r-Cuox(400) samples. Arrows in the panels indicate oxides species.

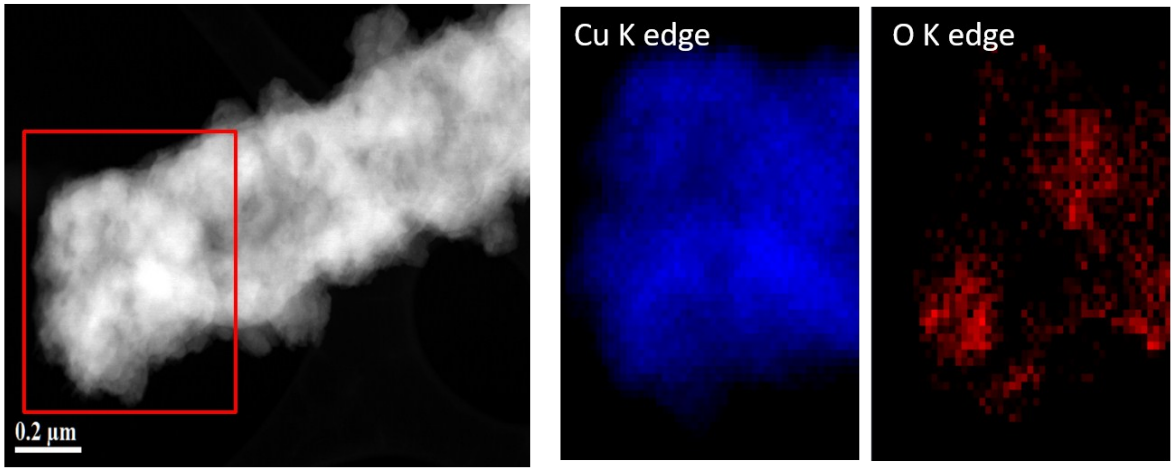

Figure S3. STEM image and corresponding electron energy loss spectroscopy mapping for the selected area.

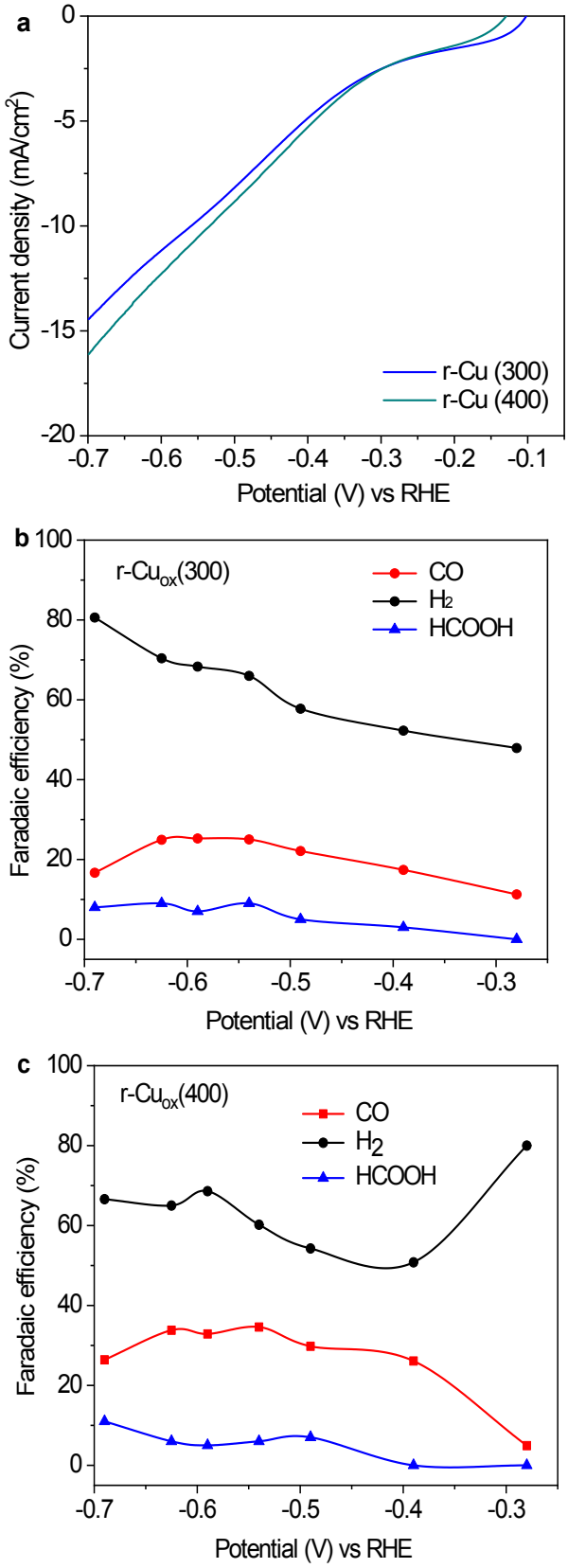

Figure S4. (a) Polarization curves and (b,c) F.E. of CO, H_2 and HCOOH as a function of the potential for the r-Cu_{ox}(300) and r-Cu_{ox}(400) samples in CO_2-satuated 0.1 M $KHCO_3$ solutions.

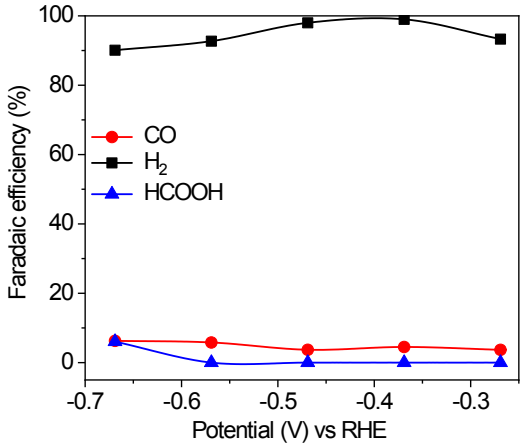

Figure S5. F.E. of CO, H_2 and HCOOH as a function of the potential for pristine Cu sample.

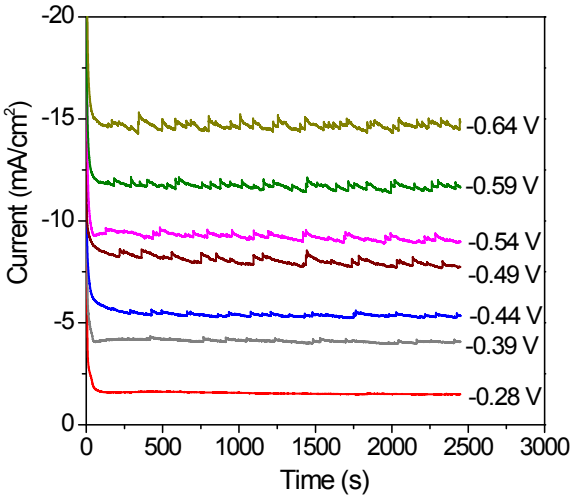

Figure S6. Current densities of the catalyst over 40 min operation at different potentials.

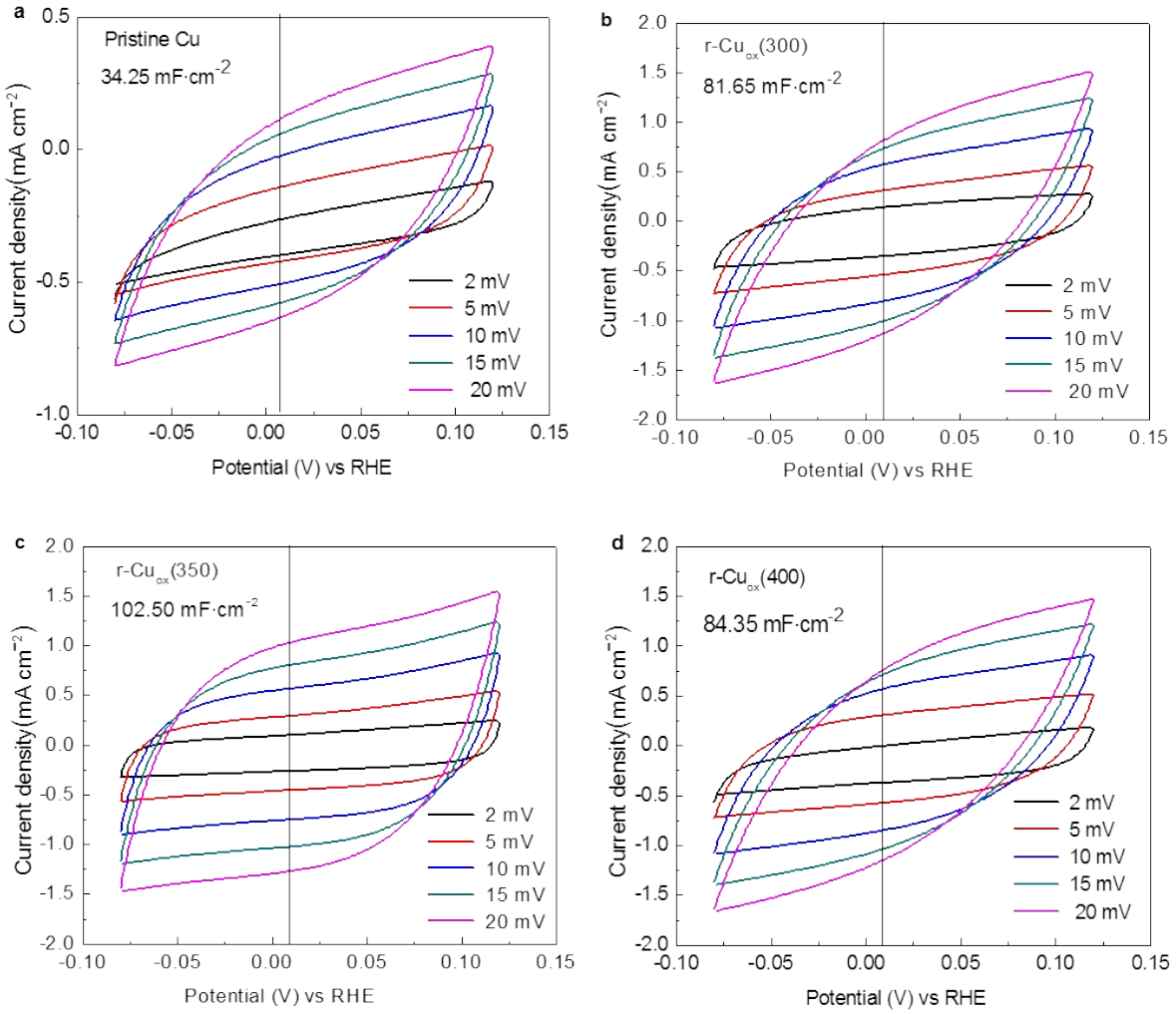

Figure S7. (a-d) Cyclic voltammetry curves for the pristine Cu, r-Cu_{ox}(300) , r-Cu_{ox}(350) and r-Cu_{ox}(400) catalysts in the potential range, in which Faradaic processes are not occurring in 0.1 M $KHCO_3$ electrolyte.

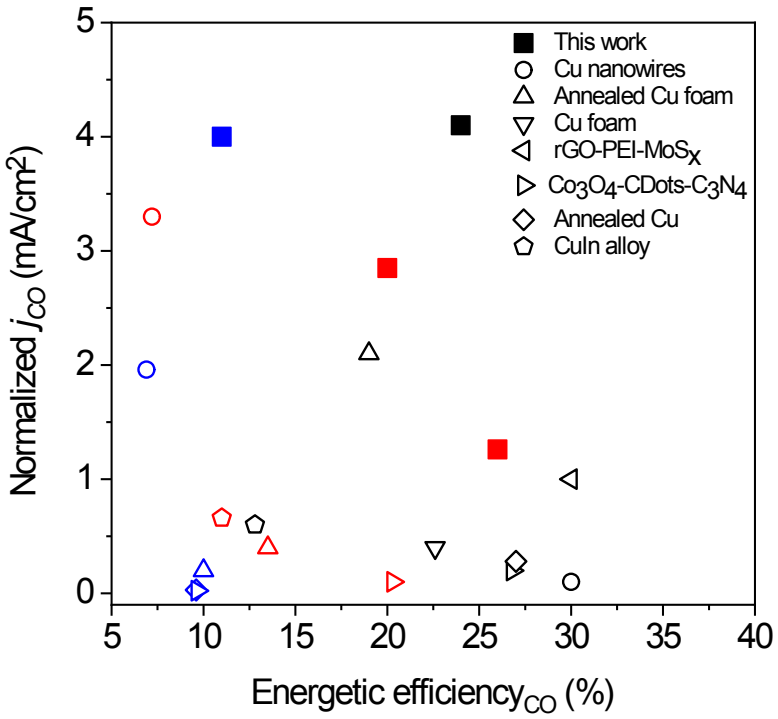

Figure S8. Comparison of $E.E._{CO}$ and j_{CO} for r-Cu_{ox}(350) with other reported syngas generation electrocatalysts. The symbols in black, red and blue stand for the syngas with H_2/CO ratio of 1, 2 and 3, respectively. The details are provided in Table S2.

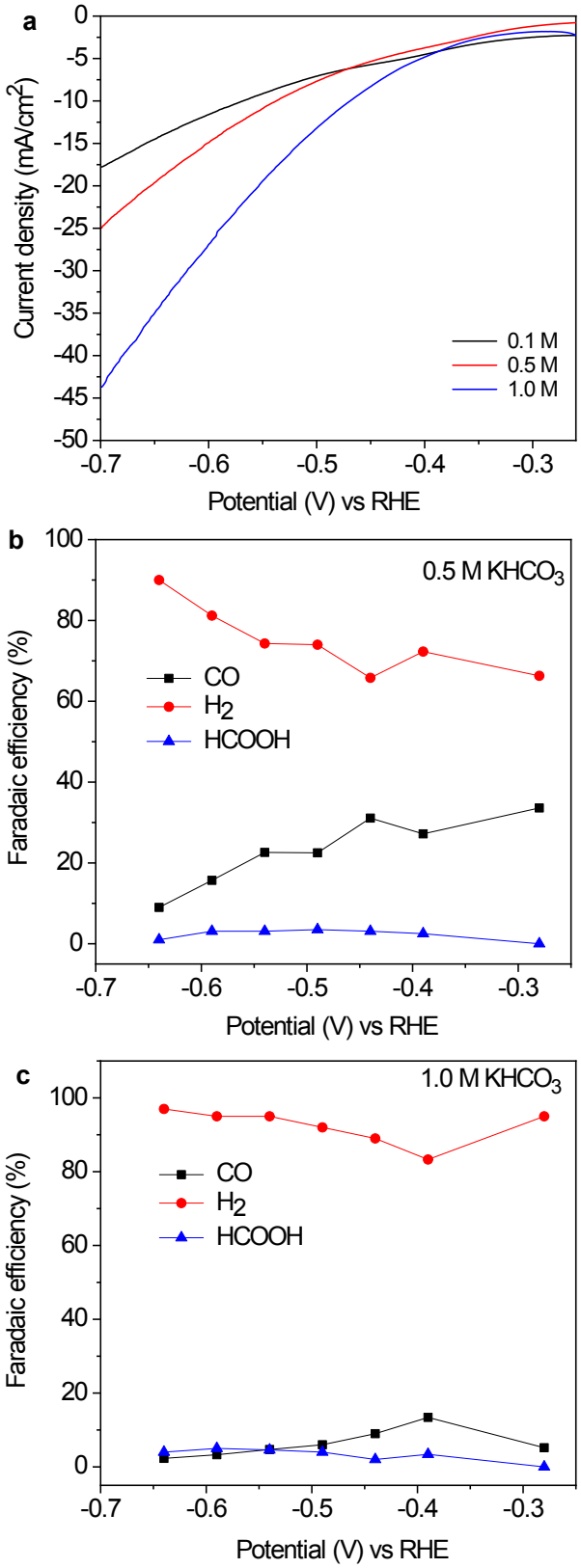

Figure S9. (a) Polarization curves and (b, c) F.E. of CO, H_2 and HCOOH as a function of the potential for r-Cu_{ox}(350) at different concentrations of CO_2-satuated $KHCO_3$ solutions.

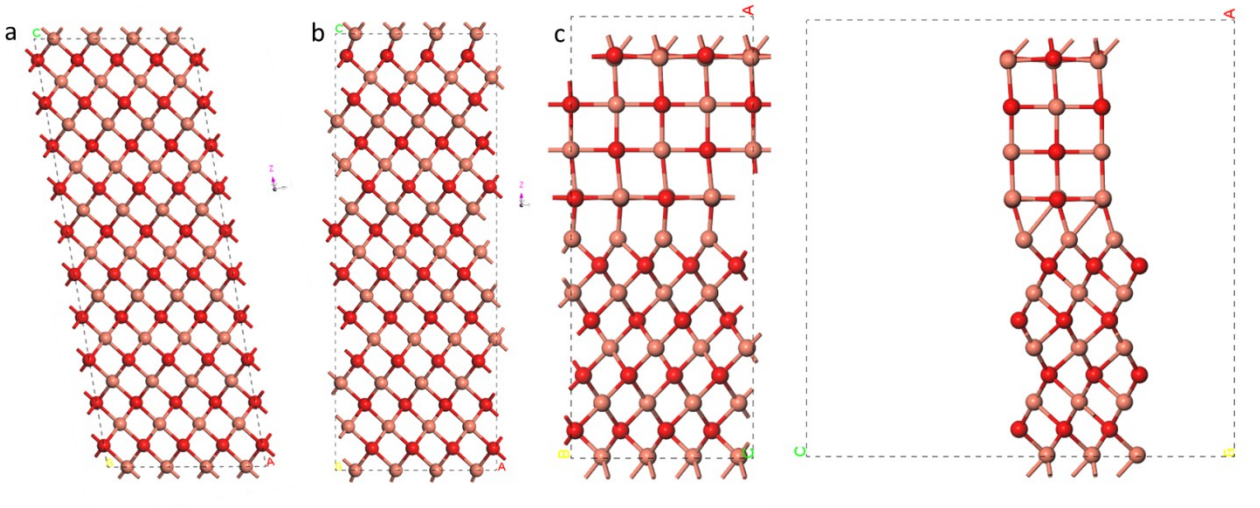

Figure S10. (a,b) m-CuO 2×1×5 supercell before and after reconstruction. (c) top view (left) and side view (right) of the constructed CuO-heterostructure. Colour code: pink, copper; red, oxygen.

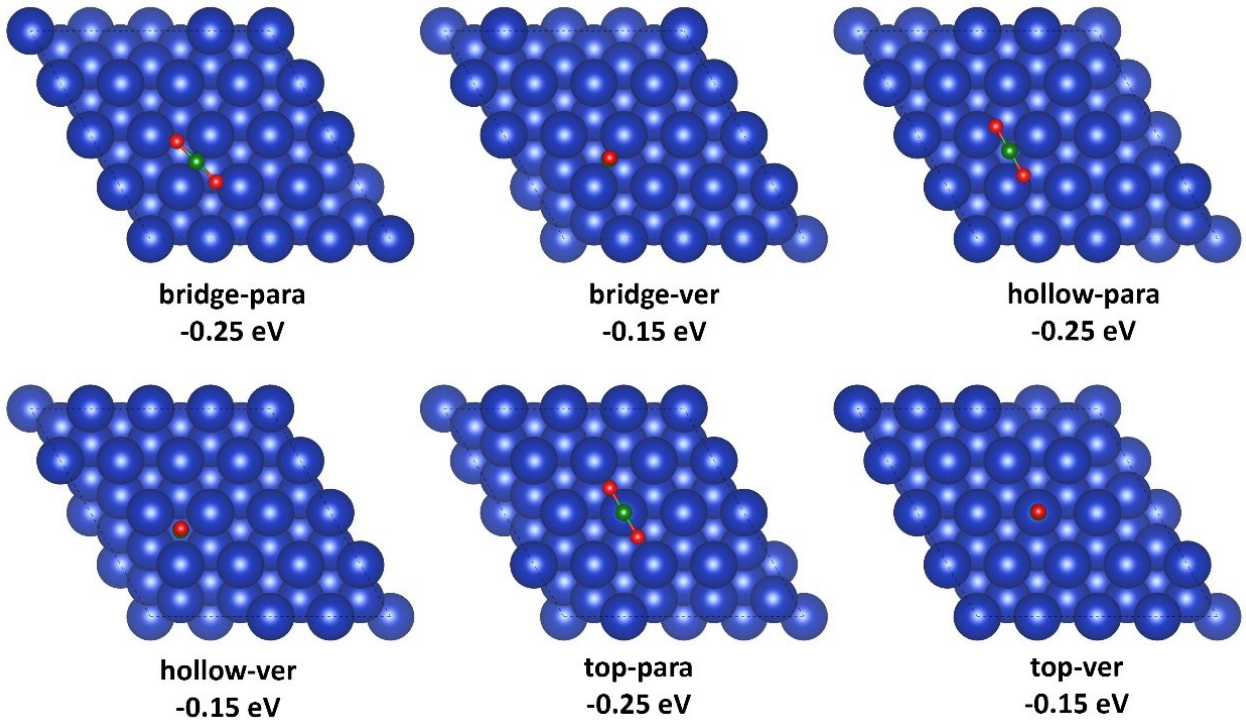

Figure S11. Different CO_2 adsorption configurations on the Cu(111) surface. For each optimized structure, the starting configuration is described as 'adsorption position-CO_2 orientation'. Colour code: blue, copper; red, oxygen in CuO; orange, oxygen in adsorbate; green, carbon; white, hydrogen.

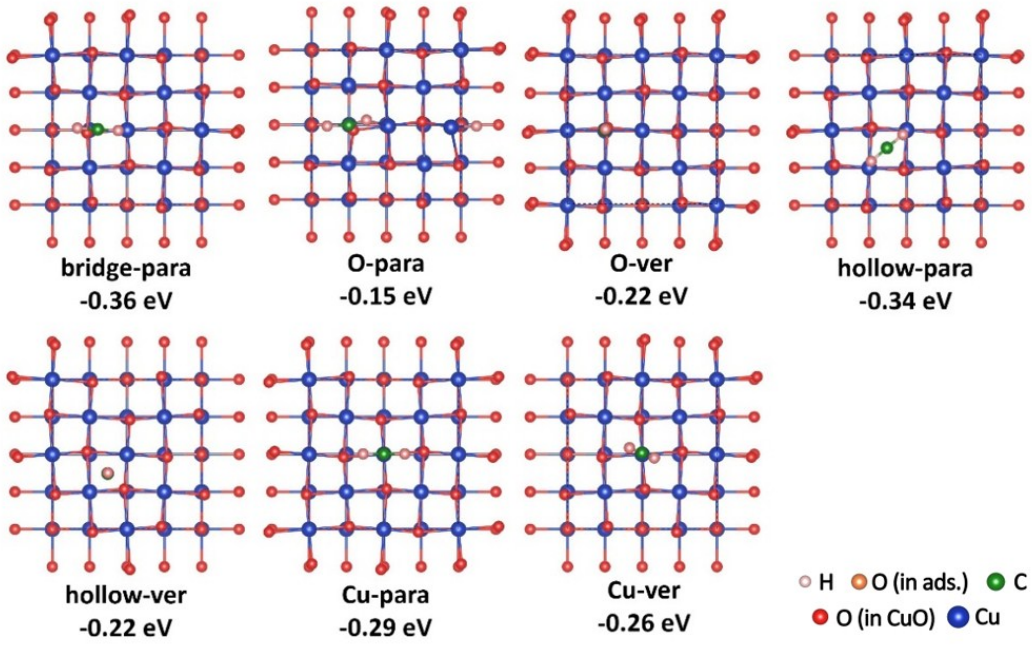

Figure S12. Different CO_2 adsorption configurations on the c-CuO(001) surface. For each optimized structure, the starting configuration is described as 'adsorption position-CO_2 orientation'.

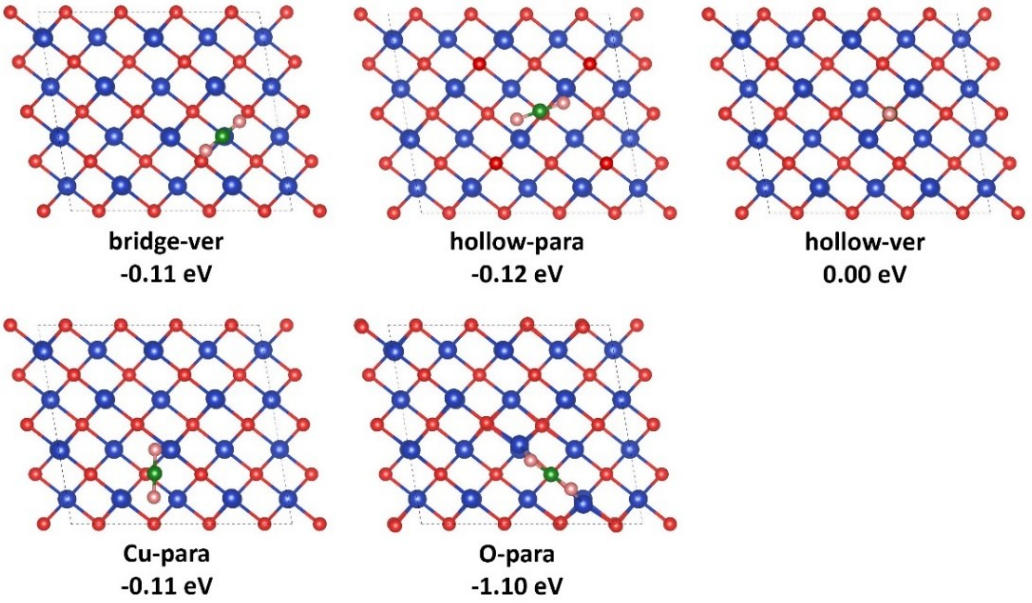

Figure S13. Different CO_2 adsorption configurations on the m-CuO(010) surface. For each optimized structure, the starting configuration is described as 'adsorption position-CO_2 orientation'. For this monoclinic structure, geometry optimization of standalone substrate did not succeed; therefore, the substrate energy is defined using the weakest CO_2 adsorption configuration (the 'hollow-ver' configuration). Color code as in Figure S12.

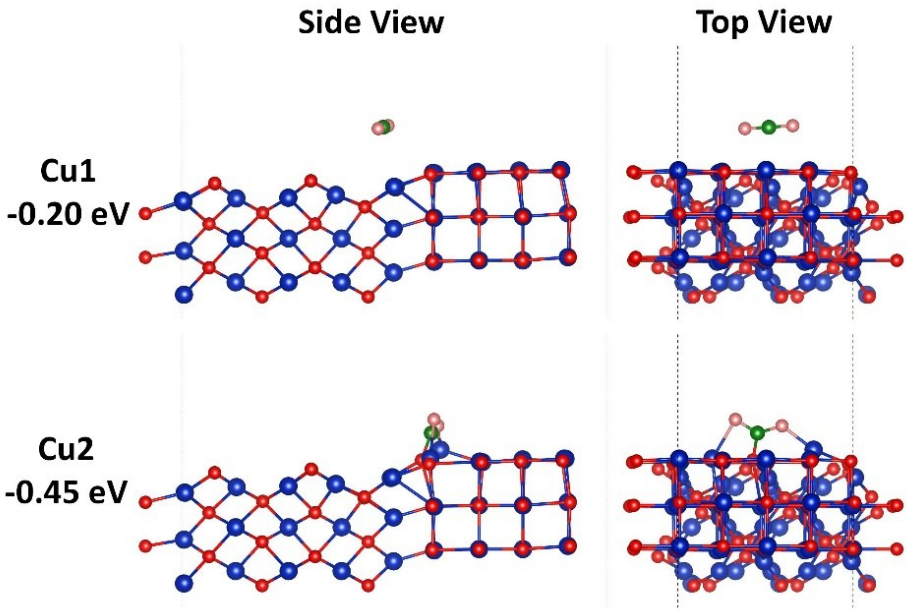

Figure S14. Different CO_2 adsorption configurations on the CuO-heterostructure. For each optimized structure, the starting configuration is described as 'adsorption position'. Color code as in Figure S12.

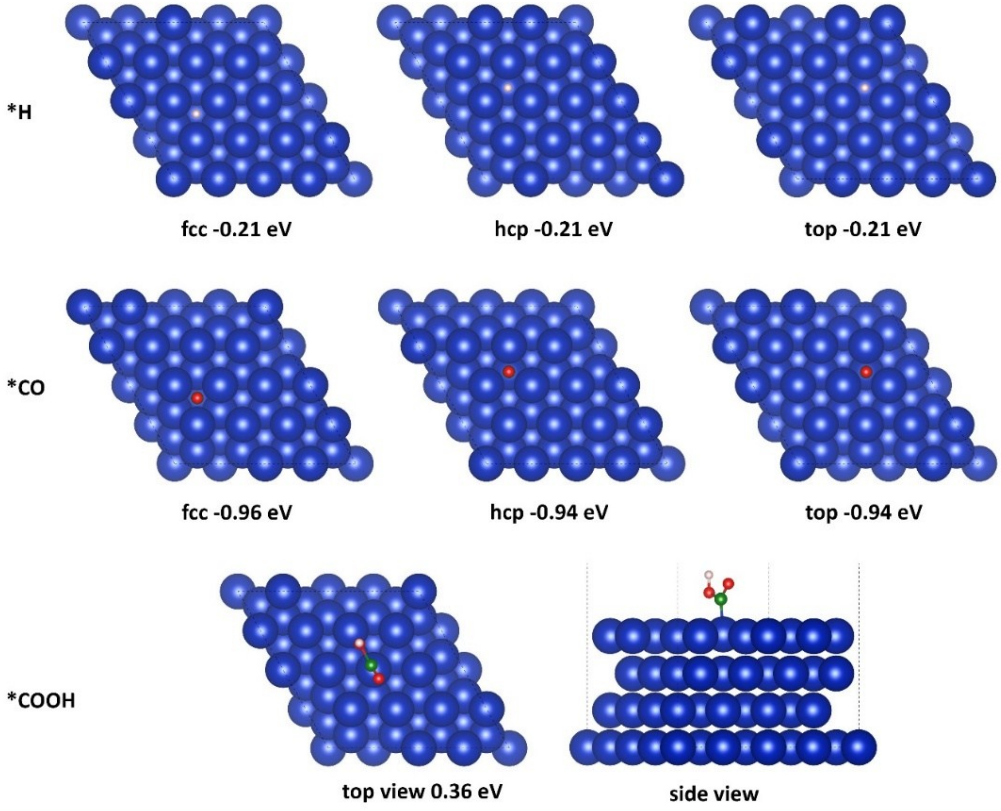

Figure S15. Different configurations of adsorption of reaction intermediates on Cu(111). Color code as in Figure S12.

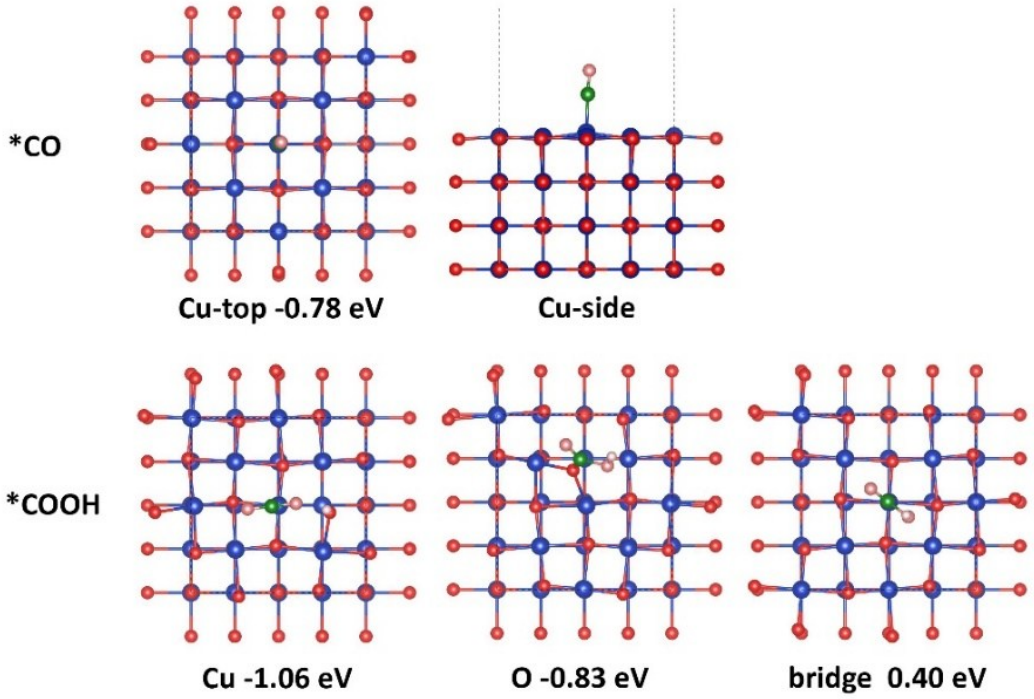

Figure S16. Different configurations of adsorption of reaction intermediates on the c-CuO(001) surface. Color code as in Figure S12.

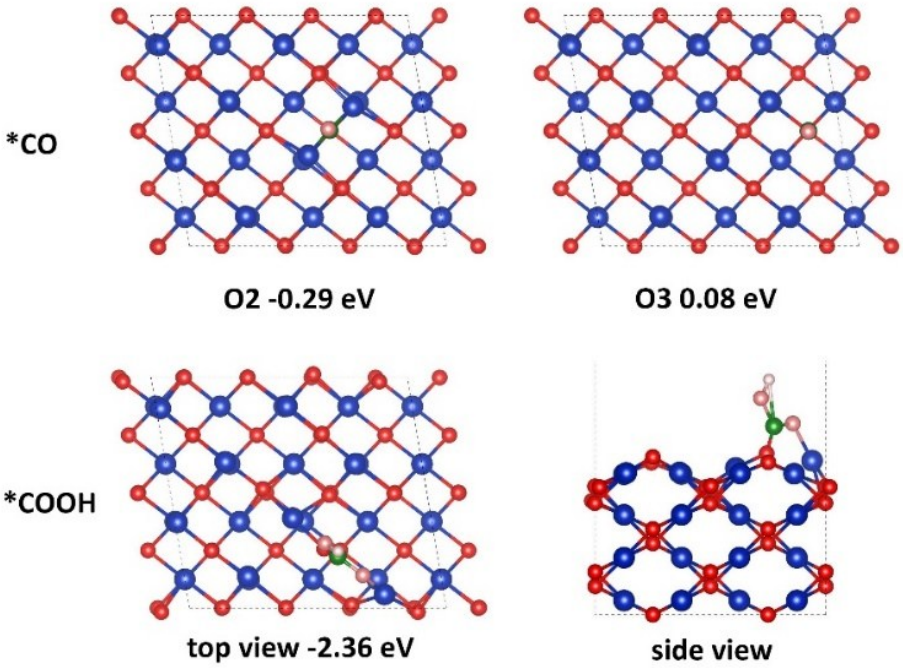

Figure S17. Different configurations of adsorption of reaction intermediates on the m-CuO(010) surface. Color code as in Figure S12.

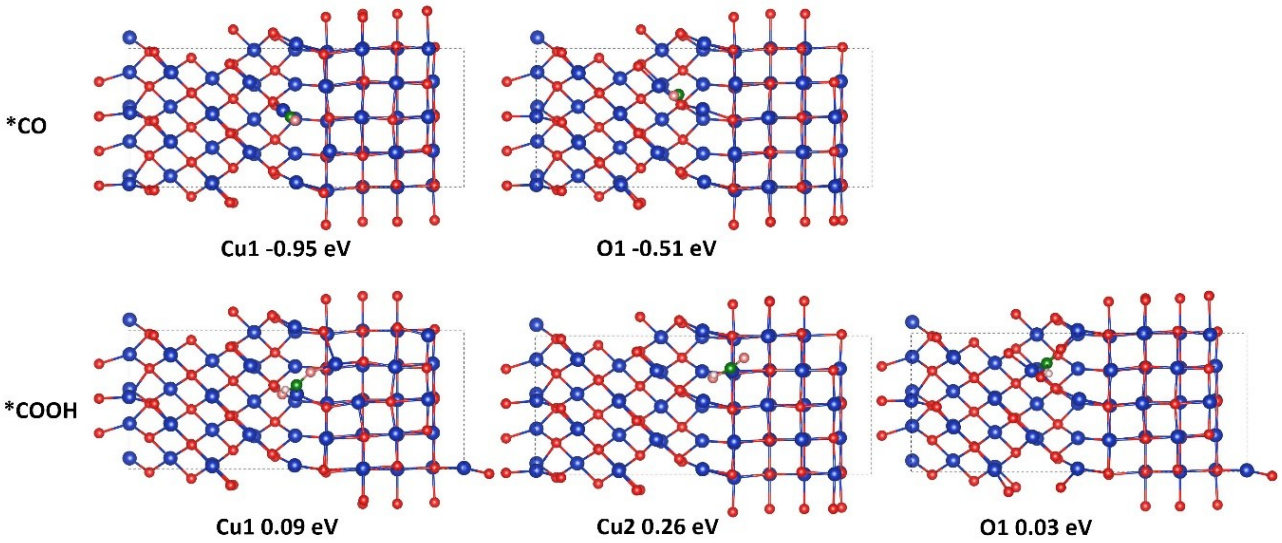

Figure S18. Different configurations of adsorption of reaction intermediates on the CuO-heterostructure. Color as in Figure S12.

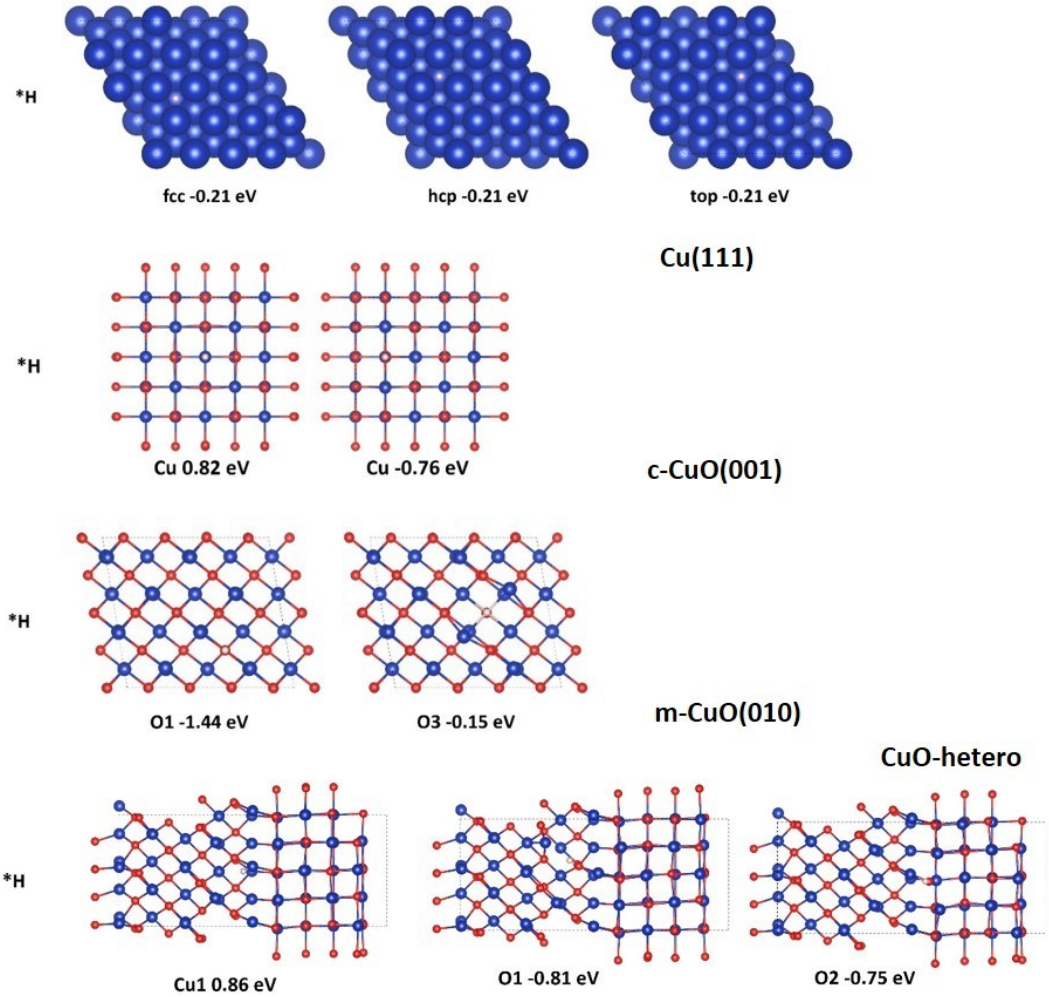

Figure S19. H* adsorption on different surfaces. Color code as in Figure S12.

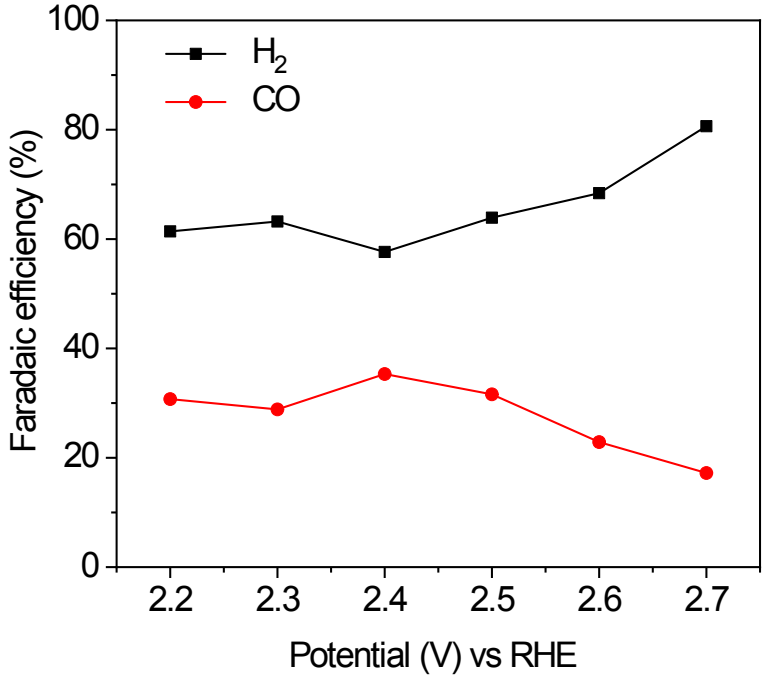

Figure S20. F.E. of CO and H_2 on r-Cu_{ox}(350) as a function of the applied voltage.

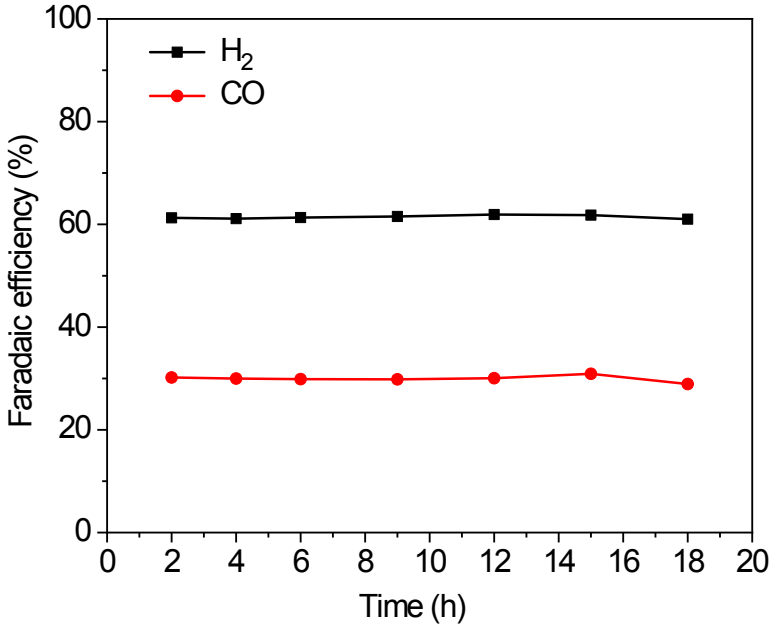

Figure S21. F.E. of CO and H_2 on r-Cu_{ox}(350) as a function of time under applied voltage of 2.2 V.

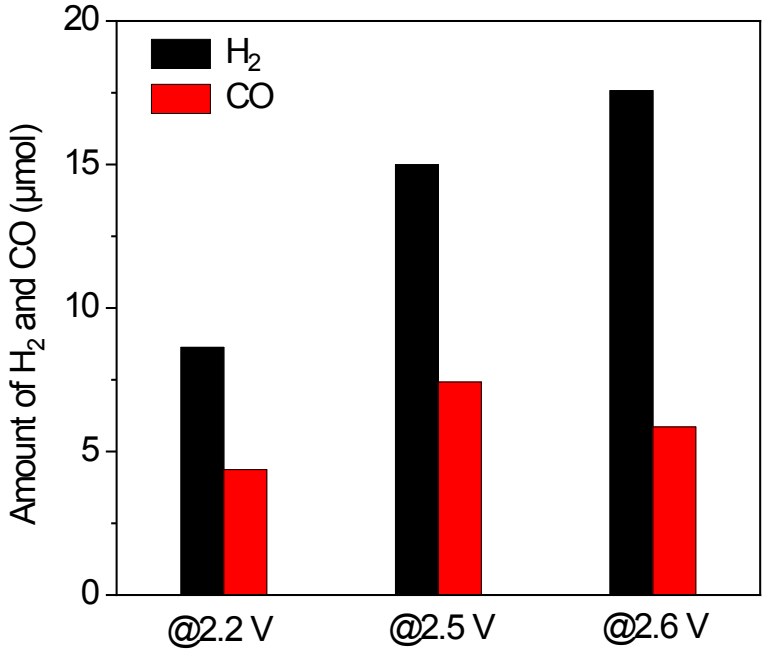

Figure S22. Amount of generated CO and H_2 using the different solar cell potentials during a 30 min electrolysis.

Supplementary Methods

Computation Models

Three bulk models were constructed in this study: Cu, cubic-CuO, and monoclinic-CuO. The corresponding lattice parameters for these bulk materials were optimized to 3.547 Å × 3.547 Å × 3.547 Å (α=β=γ=90°), 4.226 Å × 4.226 Å × 4.226 Å (α=β=γ=90°), and 4.720 Å × 3.459 Å × 5.181 Å (α=γ=90°, β=99.5°), respectively. Afterwards the surface of each bulk material was cleaved to match experimental observation of this work, as outlined in Figure 2, which are Cu(111), c-CuO(001), and m-CuO(010). The construction of heterostructure was conducted in the following way. First, a (2 × 1 × 5) m-CuO supercell (Figure S11a) was reconstructed to a cubic structure (Figure S11b) with a lattice parameter of 9.44 Å × 3.46 Å × 25.55 Å. Afterwards, the lattice of this reconstructed m-CuO supercell in *a* and *b* direction was slightly adjusted to match that of a (2 × 1 × 2) c-CuO supercell, which is 8.45 Å × 4.23 Å × 8.45 Å. Subsequently, bottom ten layers of the reconstructed m-CuO were selected to construct the heterostructure. Lastly, this periodic heterostructure was cleaved in (010) direction to construct a slab with about 15 Å vacuum space in between, as shown in Figure S11c. The length of this supercell along heterojunction direction is then further optimized to 20.47 Å.

The reaction intermediate states considered in this study include CO_2 adsorption, *COOH, *CO, and *H. Based on these calculations, the free energy diagram for two products, CO and H_2, can be summarized. The adsorption energy of CO_2 is defined as

$E_{ad} = E_{total} - (E_{substrate} + E_{CO2})$

where E_{total} is the total energy of the system with adsorbed CO_2, $E_{substrate}$ and E_{CO2} are the energy of substrate and isolated CO_2, respectively. The adsorption energy of adsorbed states, including *COOH, *CO, and *H are defined using gas phase energy as a reference (see below):

$E_{*COOH} = E_{total} - (E_{substrate} + E_{HCOOH} - ½\ E_{H2})$

$E_{*CO} = E_{total} - (E_{substrate} + E_{CO})$

$E_{*H} = E_{total} - (E_{substrate} + ½\ E_{H2})$

Supplementary Tables

Table S1. Cu K-edge EXAFS fitting results for pristine Cu, Cu350 and Cu foil.

		coordination number	Bond length	$\sigma^2(10^{-3}Å^2)$
Pristine Cu	Cu-Cu	5.9	2.55	9.3
Cu350	Cu-O	2.1	1.84	4.6
	Cu-Cu	5.7	2.55	9.6
Cu foil	Cu-Cu	12	2.54	9.1

Table S2 Comparison of the potential (V vs RHE), EE_{CO} (%) and j_{CO} (mA/cm^2) for different electrocatalysts and desired syngas with H_2/CO ratio of 1/1, 2/1 and 3/1. The labels are the same as those in Fig. S8**.**

	Catalyst	Potential（V vs RHE）	EE_{CO}(%)	j_{CO}(mA/cm^2)	H_2/CO	Ref.
■	r-Cu_{ox}(350)	-0.49	24	4.10	1/1	This work
○	Cu nanowires	-0.23	30	0.10	1/1	[1]
△	Annealed Cu foam	-0.45	19	2.10	1/1	[2]
▽	Cu foam（20s）	-0.50	22.6	0.40	1/1	[3]
◁	rGO-PEI-MOSx	-0.45	30	1.00	1/1	[4]
▷	Co_3O_4-CDots-C_3N_4	-0.45	26.8	0.20	1/1	[5]
◇	Annealed Cu	-0.35	27	0.28	1/1	[6]
⬠	CuIn alloy	-1.00	12.8	0.60	1/1	[7]
■	r-Cu_{ox}(350)	-0.28	26	1.26	2/1	This work
■	r-Cu_{ox}(350)	-0.39	20	2.85	2/1	This work
★	Pd/C	-0.50	18.1	0.10	2/1	[8]
△	Annealed Cu foam	-0.34	13.5	0.40	2/1	[2]
○	Cu nanowires	-0.58	7.2	3.30	2/1	[1]
⬠	CuIn alloy	-0.10	11	0.66	2/1	[7]
▷	Co_3O_4-CDots-C_3N_4	-0.40	20.3	0.10	2/1	[5]
■	r-Cu_{ox}(350)	-0.64	11	4.00	3/1	This work
★	Pd/C	-0.80	19	0.30	3/1	[8]
○	Cu nanowires	0.64	6.9	1.96	3/1	[1]
▷	Co_3O_4-CDots-C_3N_4	-0.35	9.6	0.03	3/1	[5]
◇	Annealed Cu	-0.20	9.65	0.02	3/1	[6]
△	Annealed Cu foam	-0.28	10	0.20	3/1	[2]

Table S3. Frequencies and thermodynamic energy corrections for different adsorbates involved in CO_2RR and HER.

Adsorbate	Frequencies (meV)	ZPE (eV)	$\int C_p dT$ (eV)	-TS (eV)
***CO**	225.76, 35.11, 29.04, 28.46, 16.60, 13.87	0.17	0.08	-0.15
***COOH**	433.31, 209.12, 147.18, 115.31, 75.28, 74.10, 42.15, 28.58, 21.27	0.57	0.05	-0.08
***H**	135.73, 101.86, 99.73	0.17	0.00	-0.01

Table S4. Frequencies and thermodynamic energy corrections for gas phase molecules.

Adsorbate	Frequencies (meV)	ZPE (eV)	$\int C_p dT$ (eV)	-TS (eV)
CO	263.60	0.13	0.10	-0.61
CO_2	293.15, 163.49, 78.49, 78.37	0.31	0.11	-0.66
HCOOH	448.89, 370.22, 218.52, 167.58, 155.83, 132.89, 123.42, 83.58, 73.98	0.89	0.11	-0.50
H_2	536.62	0.27	0.10	-0.42

References

[1] D. Raciti, K. J. Livi, C. Wang, Nano Letters 2015, 15, 6829.

[2] S. X. Min, X. L. Yang, A. Y. Lu, C. C. Tseng, M. N. Hedhili, L. J. Li, K. W. Huang, Nano Energy 2016, 27, 121.

[3] A. Dutta, M. Rahaman, N. C. Luedi, P. Broekmann, Acs Catalysis 2016, 6, 3804.

[4] F. Li, S.-F. Zhao, L. Chen, A. Khan, D. R. MacFarlane, J. Zhang, Energy & Environmental Science 2016, 9, 216.

[5] S. J. Guo, S. Q. Zhao, X. Q. Wu, H. Li, Y. J. Zhou, C. Zhu, N. J. Yang, X. Jiang, J. Gao, L. Bai, Y. Liu, Y. Lifshitz, S. T. Lee, Z. H. Kang, Nature Communications 2017, 8: 1828.

[6] C. W. Li, M. W. Kanan, Journal of the American Chemical Society 2012, 134, 7231.

[7] Z. B. Hoffman, T. S. Gray, K. B. Moraveck, T. B. Gunnoe, G. Zangari, Acs Catalysis 2017, 7, 5381.

[8] W. C. Sheng, S. Kattel, S. Y. Yao, B. H. Yan, Z. X. Liang, C. J. Hawxhurst, Q. Y. Wu, J. G. G. Chen, Energy & Environmental Science 2017, 10, 1180.